Accepted to *Journal of Computational Physics*

Stability and Convergence Analysis of a Dynamics-based Collective Method for Random Sphere Packing

Yanheng Li and Wei Ji*
Department of Mechanical, Aerospace and Nuclear Engineering
Rensselaer Polytechnic Institute
110 8th Street, JEC 5040 MANE, Troy, NY 12180
*Corresponding author, jiw2@rpi.edu

Abstract

The simulation of granular materials requires an initial overlap-free packing of spherical particles at high volume packing fractions. In previous work, a dynamics-based collective approach, the Quasi-Dynamics Method (QDM), has been proposed to generate densely distributed spheres in an enclosed container. However, the stability and efficiency of the QDM were not fully addressed. In this paper, the algorithm is reformulated with two control parameters and the impact of these parameters on the algorithm performance is investigated. First, theoretical analyses and numerical verifications for extreme 1-D/2-D packing systems are conducted and the range of the control parameters in which the algorithm is convergent is analytically determined. Then, the analysis is extended to 3-D packing systems and the estimation of the parameter range is verified numerically. Finally, the algorithm is applied to modeling a cylindrical 3-D packing system and the convergence performance at different volume packing fractions is studied. Results show that the QDM is highly efficient in packing spheres at volume packing fractions that are close to the random close packing limit.

Key Words: Granular material, Random sphere packing, Quasi-Dynamics method, Stability analysis, Convergence rate, Packing fraction distribution

1. Introduction

The modeling and simulation of random sphere packing play important roles in the study of granular material behavior in many scientific and engineering systems [1, 2]. These systems span different length scales in practice, from a microscopic scale, such as the micro-structure evolution of glass, to a macroscopic scale, such as the pebble flow in Pebble Bed Reactors (PBRs) [3, 4]. To study the dynamic behavior of the granular material in these systems, a key step is to obtain a realistic packing arrangement of granular materials. For example, as the first step of pebble flow simulations in a PBR, an initial and static pebble packing configuration is needed [5, 6]. This step can be viewed as a classic random sphere packing problem, where mono-sized hard spheres are densely arranged within a confined space (usually a container). Many random sphere packing algorithms have been developed to solve this problem. In practical applications, the development of random sphere packing methods may face great computational challenges. The challenges can be in two fold. First, the studied

sphere packing system may be at a large scale and contain a large number of spherical particles. For example, there are a total of about 450,000 pebbles in the PBMR-400 pebble bed reactor design. It is desirable to have a highly efficient packing method that can provide a random arrangement of pebbles for reactor physics analysis on the routine basis. Second, a rigorous theoretical foundation is needed to provide a guideline for the utilization of developed packing methods, such as under what conditions the method can provide highest stability and efficiency. This is especially significant for designers or analysts when they apply a packing algorithm to the study of a granular material system. Currently, such a theoretical analysis is usually lacking for most existing random sphere packing methods, which were detailed on how they work but not on why they work. We aim to address such a research gap in this paper by analyzing a previously developed random sphere packing method and expect to bring this research direction to the sphere packing research community's attention.

Computer simulation of random sphere packing has been studied for a long time [7-17], and many numerical algorithms and strategies have been developed. Based on sphere generation strategies, these algorithms can be categorized as sequential or collective packing methods [11, 13, 16]. In the sequential packing methods, spheres are added into a domain one-by-one [18], or group-by-group [1], and a non-overlapping rule is enforced throughout the insertion process. In the collective packing methods, spheres are first inserted into a domain allowing sphere overlaps and a collective sphere position rearrangement or sphere size adjustment is performed to eliminate overlaps [10, 11]. Although the sequential strategy usually has a high efficiency and is widely adopted [1], it cannot effectively control the total insertions and the volume packing fraction, which is necessary for some applications such as the pebble packing in PBRs. The collective strategy is normally not as fast and simple as the sequential method, but can adequately control the total sphere number and hence the volume packing fraction. The collective methods are usually used to pack spheres at high volume packing fractions, such as obtaining random close packing (RCP) for the study of sphere jamming phenomenon [17]. Based on physical models used in packing spheres, packing algorithms can also be divided into dynamics-based methods and non-dynamics-based methods. In the dynamics-based methods, such as the sequential gravitational deposition method [19], the optimized Monte Carlo method based on the Lennard–Jones potential and Morse potential [20], or the collective discrete element method (DEM) [1, 3], realistic forces are adopted to implement an arrangement. The resultant sphere packing configuration can therefore be more realistic [21]. However, most dynamics-based methods are not efficient and even worse when the packing approaches the RCP state [11]. On the contrary, the non-dynamics-based methods rearrange the packing configuration by purely mathematical manipulations without any physical consideration, such as the domain triangulation [1] or mathematical optimization methods [22]. These methods generally have better efficiency at a high packing fraction range that is close to RCP but the realistic fidelity is normally lost. In the realistic configuration of granular material systems, such as in PBRs, the spheres are stacked at around 61%~62% volume packing fractions and forces exist between spheres and between spheres and walls. In order to provide an initial packing configuration that has a similar packing fraction distribution to the realistic configuration and takes into account the actual

physical forces, a collective dynamics-based method is needed for the initial packing of granular materials.

In the previous work [21], the Quasi-Dynamics Method (QDM), a collective dynamics-based method, has been developed. Different from other existing collective packing methods, which were developed to find the maximally-dense arrangement (or named a RCP configuration) of spheres within a given volume [10, 11, 13, 16, 23], the QDM was developed for the application to analyzing pebble flows in PBRs by providing an initial pebble packing, which is less dense than the RCP. It has been demonstrated that such an initial packing is important in speeding up the pebble flow simulation to reach an equilibrium state [5, 21]. In the QDM, the positions of the predetermined number of pebbles are first generated by a uniform sampling procedure allowing pebble overlaps. Then an efficient overlap elimination process is applied based on a simplified normal contact force model. The basic idea of the QDM is the same as all other collective rearrangement methods: start with an overlapped configuration and then apply an overlap removal procedure. The difference lies in how to move the spheres apart to a final overlap-free configuration. The unique feature of the QDM is the employment of a simplified normal contact force model while most other collective methods are based on purely geometrical manipulations or fully realistic physics that is more than needed for an initial packing. It has shown that the developed QDM can successfully provide a fast packing for a PBR design in both cylindrical and annular geometries [21]. This method can be extended to analyze a general granular flow simulation by efficiently providing an initial and static random sphere packing configuration. It was found, however, that the stability and efficiency of the developed method depend on user-defined parameters and how to choose these parameters for an optimal performance is still unknown. In addition, volume packing fraction was demonstrated to have a great influence on the algorithm convergence. These issues were not fully addressed and analyzed yet and answers to these questions would provide a theoretical guideline in the utilization of the method for analyzing actual granular material systems. More important, since the QDM is a collective packing method, the approach to analyze the QDM can be naturally extended to analyze other collective rearrangement algorithms. These formulate the objective of current research presented in this paper.

First, the QDM is reformulated into a two-parameter form, and the impact of these two control parameters on the algorithm performance is analyzed through extreme cases in 1-D and 2-D geometries which represent the smallest and largest close packing systems. Then, the conclusion from 1-D and 2-D situations is extended and verified numerically in 3-D geometry. For the packing fraction impact, the numerical results show that the QDM works efficiently for the packing fractions below 63%, which is within the realistic PBR packing fraction range [4]. The algorithm can handle packing fractions up to around 64%, which is approximately the random close packing (or more precisely, maximally random jamming) state [14, 17]. For packing fractions higher than this value, since local jamming widely exists, the algorithm is hardly converging. Certain techniques, such as vibration, are needed to shift the spheres out of the jammed state.

2. Reformulation of the Quasi-Dynamics Methods (QDM)

In the Quasi-Dynamics Method (QDM), the basic idea is regarding the sphere-to-sphere overlap as a compressed spring system. After all the spheres are initially positioned by uniformly sampling each sphere's center position in a container, overlaps between spheres exist due to the finite size of spheres. A sphere bears repulsive forces from all other overlapped spheres. Each force points to the center of the sphere in question along the center-to-center direction and its magnitude is determined by the overlap size. The total net repulsive force, i.e. the summation of each repulsive force from overlapped spheres, determines the direction and distance to move the sphere. In the QDM, the moving distance is assumed proportional to the magnitude of the total net force. During the overlap elimination, if a sphere overlaps with the container wall, the wall-to-sphere repulsive force is calculated in a similar way. The general procedure of the QDM has been described in the previous paper [21] and is summarized below:

For two overlapped spheres i and j, located at $\boldsymbol{X}_\mathrm{i}$, $\boldsymbol{X}_\mathrm{j}$, with radii r_i and r_j, the overlap size δ_ij is defined as $r_\mathrm{i}+r_\mathrm{j}-\|\boldsymbol{X}_\mathrm{i}-\boldsymbol{X}_\mathrm{j}\|$. The repulsive force acted on sphere i is calculated by:

$$\boldsymbol{F}_{\mathrm{n,ij}} = K_\mathrm{p}\sqrt{r_\mathrm{ij}}\delta_\mathrm{ij}\boldsymbol{n}_\mathrm{ij}, \tag{1}$$

where $r_\mathrm{ij}= r_\mathrm{i}r_\mathrm{j}/(r_\mathrm{i}+r_\mathrm{j})$, K_p is a constant associated with the sphere elastic constant, and $\boldsymbol{n}_\mathrm{ij}$ is a unit normal vector defined as $(\boldsymbol{X}_\mathrm{i}-\boldsymbol{X}_\mathrm{j})/\|\boldsymbol{X}_\mathrm{i}-\boldsymbol{X}_\mathrm{j}\|$. Let M_i be the set of all spheres that overlap with sphere i, the total repulsive force $\boldsymbol{F}_\mathrm{i}$ acting on sphere i is the vector summation of $\boldsymbol{F}_\mathrm{n,ij}$ over all M_i spheres:

$$\boldsymbol{F}_\mathrm{i} = \sum_{j\in M_i}\boldsymbol{F}_{\mathrm{n,ij}} = \sum_{j\in M_i} K_\mathrm{p}\sqrt{r_\mathrm{ij}}\delta_\mathrm{ij}\boldsymbol{n}_\mathrm{ij}. \tag{2}$$

Similarly, if a sphere overlaps with the wall boundary and the overlap size is δ_wi, the repulsive wall-to-sphere contact force $\boldsymbol{W}_\mathrm{i}$ is calculated by:

$$\boldsymbol{W}_\mathrm{i} = K_\mathrm{w}\sqrt{r}_\mathrm{i}\delta_\mathrm{wi}\boldsymbol{n}_\mathrm{wi}, \tag{3}$$

where K_w is a constant associated with the wall elasticity, and $\boldsymbol{n}_\mathrm{wi}$ is an inner unit normal vector from the wall.

The displacement of the sphere is calculated by:

$$\Delta\boldsymbol{X}_i = K_\mathrm{V}\left(\boldsymbol{F}_\mathrm{i}+\boldsymbol{W}_\mathrm{i}\right)\Big/r_\mathrm{i}^3 = K_\mathrm{V}\left(\sum_{j\in M_i} K_\mathrm{p}\sqrt{r_\mathrm{ij}}\delta_\mathrm{ij}\boldsymbol{n}_\mathrm{ij} + K_\mathrm{w}\sqrt{r}_\mathrm{i}\delta_\mathrm{wi}\boldsymbol{n}_\mathrm{wi}\right)\Big/r_\mathrm{i}^3, \tag{4}$$

where K_v is a constant determined by users .

In the QDM, the overlap elimination process is performed iteratively for each sphere based on Eqs. (1)-(4) until no overlap exists. The optimal convergence performance can be obtained by adjusting the constants K_p, K_w, and K_v. However, how to select these constants to 1) guarantee the convergence, and 2) obtain the best convergence rate, remains unknown and is the major task in this paper.

To simplify the analysis, we only analyze the system packed with mono-sized spheres, which is a typical configuration for granular materials in many applications, such as the PBR design in nuclear energy engineering. However, the QDM can also be applied to pack poly-sized sphere systems as a general collective packing method.

For mono-sized sphere systems, r_i and r_{ij} become constants, Eq. (4) can be further simplified as:

$$\Delta \boldsymbol{X}_i = \alpha \left(\sum_{j=1}^{M} \delta_{ij} \boldsymbol{n}_{ij} + \beta \delta_{wi} \boldsymbol{n}_{wi} \right), \tag{5}$$

where α and β are two control parameters that determine the algorithm stability and efficiency. The parameter α is a measure of the moving distance, i.e. step size at each iteration and β is the relative wall-to-sphere stiffness. In practice, the value of β is set to be greater than 2 so the wall exerts higher repulsive forces than spheres. Therefore, spheres are more easily pushed into the interior region of the container. By utilizing α and β, it equivalently simplifies the sphere-to-sphere repulsive force as:

$$\boldsymbol{F}_{n,ij} = \delta_{ij} \boldsymbol{n}_{ij}, \tag{6}$$

and the wall-to-sphere repulsive force as:

$$\boldsymbol{W}_i = \beta \delta_{wi} \boldsymbol{n}_{wi}. \tag{7}$$

To measure the convergence of the algorithm, two quantities can be used as the convergence criterion: the maximum overlap and the average overlap at each step of the iteration. In general, these two quantities may present oscillating behavior as the iteration step k increases, which will be shown in the later sections. As long as the step-average values of these two quantities decrease as k increases, the algorithm is considered to be convergent. Otherwise, the algorithm is not stable (divergent) or stabilizes at a jamming state without leading to an overlap-free configuration. In practice, it is found that the algorithm stability and convergence performance is not only determined by the control parameters α and β, but also related to the system packing fraction, geometry size, boundary constraint type, and the initial

spheres' distribution (with initial overlaps) by the uniform sampling. Due to these complications and uncertainties, it is impossible to precisely derive the range of the control parameters in which the QDM is convergent, nor is there a simple way to use other traditional approach, such as the Lyapunov function method [24], to analyze the stability range. However, by studying several 1-D and 2-D sphere packing systems, which represent some typical extreme packing states in 3-D cases, some strict analytical relationship can be derived and may provide insightful understanding of the algorithm for better performance in the application for 3-D packing systems.

In the following sections, the impact of the control parameters (especially α) on the QDM stability and efficiency will be discussed via the theoretical and numerical approaches. Furthermore, the impact of the packing fraction on the QDM convergence is also presented through numerical analysis.

3. Stability Analysis of the QDM

The stability of any collective sphere packing algorithm can be roughly defined as the extent that small sphere overlaps induced by any small perturbation on the packed system will not lead to large sphere move. The convergence of the system can be further defined as a more strict (asymptotic) stability, in which the algorithm can achieve an overlap-free configuration. The control parameters, α and β, both affect the algorithm convergence and efficiency, although they impact the QDM performance to different extents. In practice, it is observed that the impact from β is much smaller than that from α (which can be verified via both numerical and theoretical approaches later), therefore we will mainly focus on the impact from the step size α. For a general packing system, it is expected that the algorithm efficiency will be enhanced as α is increased since most overlaps can be eliminated quickly. However, if α is too large, there may be more overlaps generated compared to the previous step, causing reduced stability margin or even divergence. A critical value α_c is expected to exist such that the QDM is unstable if $\alpha>\alpha_c$. In order to determine this critical value for the sphere packing system, several simple extreme 1-D and 2-D densely packed systems are studied first under both fixed boundary and periodic boundary conditions. The fixed boundary geometry corresponds to the smallest possible constrained multi-sphere packing system assuming that spheres can only be packed horizontally, and the periodic boundary system corresponds to the largest system with an infinite number of spheres packed in an infinite system. If the QDM is applied to pack spheres in these systems given an arbitrary initial packing with overlaps, questions on how the parameters α and β affect the convergence to the overlap free configuration and what is the critical value α_c, can all be answered analytically. These analytical results are meaningful as the guideline for choosing proper control parameter that can achieve high efficiency while keep reasonable stability margin.

Due to the complexity of higher dimensional systems, the stability analysis starts with simple closely packed 1-D two-sphere systems. Each sphere has a radius r, and when there is no overlap (the system is in its final equilibrium state), the $4r$-wide 1-D container can be exactly filled by two spheres. Figure 1a shows a system with fixed boundary condition (FBC) and

Fig. 1b shows a periodic boundary condition (PBC) system. For the relative wall stiffness β under FBC, it is fixed at a value greater than 2 in order to ensure that average sphere-wall overlap is smaller than the average inter-sphere overlap. To evaluate the QDM stability in packing spheres in these systems, we start with the configuration where two spheres are in the overlap-free state, as shown in the left figures in Fig. 1. After an arbitrary small perturbation is applied to each sphere, an overlapped sphere system is obtained, as shown in the right figures in Fig. 1. We then apply QDM to perform the overlap elimination process to analyze the motions of two spheres. Sphere 1 is perturbed to the right by an arbitrary distance $\gamma\delta_0$ from the equilibrium position and sphere 2 is perturbed by $(1\text{-}\gamma)\delta_0$ to the left, where $0.5 \leqslant \gamma \leqslant 1$ (sphere 2 is closer to the boundary at its initial position) and $\delta_0 < r$. It is obvious that the resultant overlap between spheres 1 and 2 is δ_0. It should also be noted that the value of γ can also be chosen as $0 \leqslant \gamma < 0.5$, which stands for the situation that sphere 1 is closer to the boundary at its initial position and can be analyzed by the same approach as for the situation of $0.5 \leqslant \gamma \leqslant 1$. Analytical approach will be used to find out the critical value α_c so that for any chosen $\alpha < \alpha_c$, the QDM algorithm can move the perturbed spheres (which is a representation of an arbitrary initial packing system with overlaps) back to the equilibrium state under both boundary conditions. Under critical value α_c, the system is neither convergent nor divergent when the QDM is applied. It can predict that the overlap between two spheres will hold constant or periodically constant as iteration proceeds, which is defined as a critical stable state.

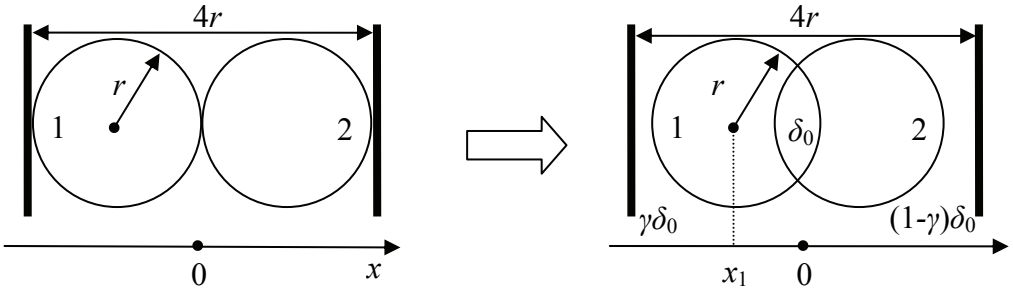

Equilibrium state configuration

Perturbed configuration (representation of an arbitrary initial configuration with overlaps)

(a) Close packing of two spheres in a 1-D system with fixed boundary condition, representing the smallest 1-D packing system

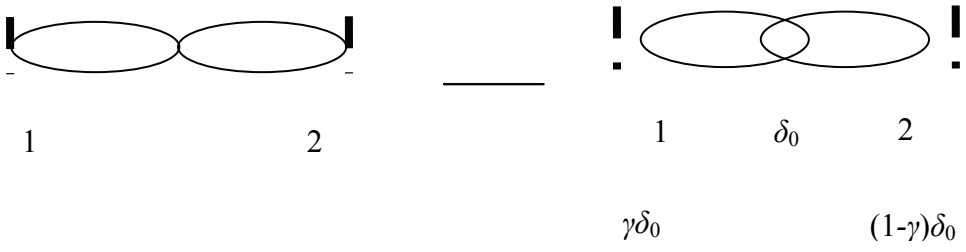

(b) Close packing of two spheres in a 1-D system with periodic boundary condition, representing the largest 1-D packing system

Fig. 1. Close packing in 1-D two-sphere systems with fixed and periodic boundary conditions. δ_0 represents an initial overlap size between two spheres and γ represents the fraction of the perturbation from sphere 1 that causes the initial overlap.

The fixed boundary case (Fig. 1a) is studied first. In the FBC system, it is observed that two possible motion modes, A and B, exist during the overlap elimination process by the QDM algorithm, as shown in Fig. 2. Under critical stable states, two spheres will follow these two modes without converging to overlap-free state and oscillate around each equilibrium position without damping. Under convergent or divergent states, two spheres will also follow these two modes but oscillations around the each equilibrium positions are dampened or increased as the iteration proceeds.

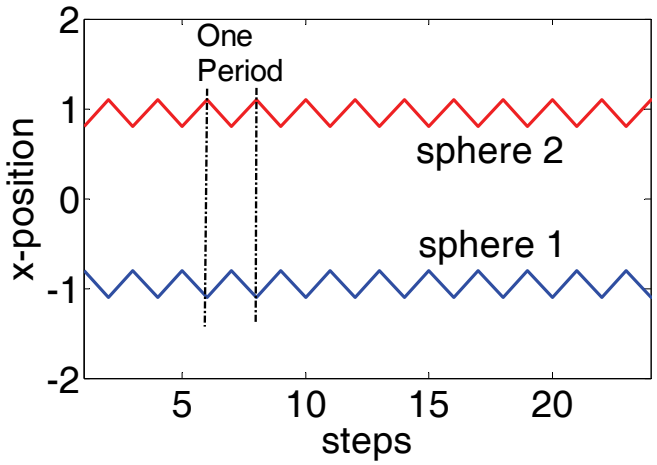

(a) Motion mode A: 2-stage cycles. Two spheres are moved always in the opposite directions at each iteration step due to the sphere-to-sphere overlap and sphere-to-wall overlap that appear alternately. Each sphere experiences the same type of overlap at each iteration step. The positions of each sphere are plotted as a function of iteration step. The figure is based on the numerical calculation with an initial perturbation δ_0=0.4 and an initial gamma value 0.5.

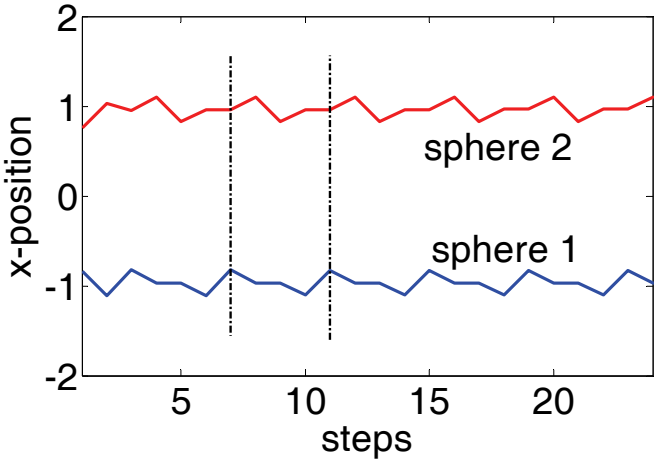

(b) Motion mode B: four-stage cycles. Each sphere experiences a four type of overlaps in each cycle but with different sequence. One sphere experiences: sphere-to-sphere overlap (1) -> sphere-to-wall overlap (2) -> sphere-to-sphere overlap (3) -> overlap free (4) ->

sphere-to-sphere overlap (1) etc. and the other experiences: sphere-to-sphere overlap (1') -> overlap free (2') -> sphere-to-sphere overlap (3') -> sphere-to-wall overlap (4') -> sphere-to-sphere overlap (1') etc. The figure is based on the numerical calculation with an initial perturbation δ_0=0.4 and an initial gamma value 0.48.

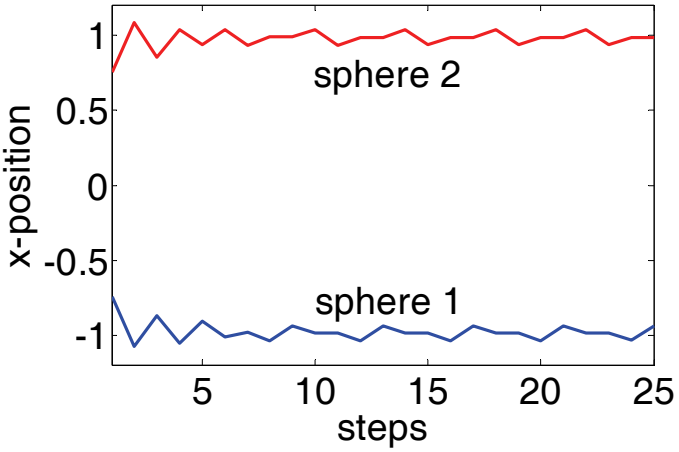

(c) General case: Starting with mode A then mode B. The figure is based on the numerical calculation with an initial perturbation δ_0=0.4 and an initial gamma value 0.2.

Fig. 2. Different motion modes for FBC systems when the QDM is applied to eliminate the overlaps between two spheres in closely packed 1-D two-sphere systems. In all the figures, α=0.66 and β=4.

For the motion mode A, it can appear only if γ=0.5. Two spheres first overlap with each other and do not overlap with the wall, and the contact force will drive two spheres to move apart. For $0<\alpha\leq 0.5$, two spheres will not overlap with the wall after the separation, and the system can approach its equilibrium state within the required tolerance in a finite number of steps. For larger α, the separation will result in overlaps with the wall. The wall overlaps push the spheres inward and make them overlap with each other again (Fig. 2a). So the motion mode A is a two-stage cycle.

For any $\gamma\neq 0.5$, the sphere motion will be mode B (Fig. 2b), or starting with mode A but change into mode B (Fig. 2c). For mode B, a cycle consists of four-stages:
1) Two spheres are separated apart by the contact force due to the initial overlap. After the separation, one sphere has an overlap with the wall (without loss of generality, assume it is sphere 2), while the other one (assume sphere 1) is overlap free;
2) Sphere 2 will move inward due to the wall overlap, while sphere 1 will stay still. After the moving, the two spheres are overlapped again;
3) Two spheres will be separated by the new inter-sphere overlap. Now sphere 1 has an overlap with the wall, while sphere 2 does not.
4) Sphere 1 will be pushed back by the wall, while sphere 2 will stay still.

We can see that because motion mode B has more stages, it can be considered as a general case, while mode A can be considered as a trivial (singular) situation. It should be noted that, for any initial condition, the sphere motion will keep following mode A if and only if γ=0.5, otherwise the sphere motion will either follow mode B, or firstly have a few cycle of mode A motion, then move following mode B (Fig. 2c). Under the critical stable condition, the motion can only be either mode A or mode B. The idea to find out the critical α value is realized by assuming that the sphere motion mode (either A or B) is strictly periodic. This is a representation of a critical stable state, and by using this assumption, the critical value α_c can be obtained.

The necessary condition to sustain mode A is γ=0.5, meaning that both spheres have equal distance to the nearest wall, which is $0.5\delta_0$. Due to symmetry, the critical value α_c can be obtained by analyzing sphere 1's consequent motions by the QDM. The initial position for sphere 1 is $x_1^{(0)}$=-r+δ_0/2. Assume that α is large enough (>1/2), after the first step, sphere 1 is moved to an updated position $x_1^{(1)}$=-r+(1/2-α)δ_0 and the overlap between two spheres disappears. However, new overlap with the left wall (boundary) appears: $\delta_{1w}^{(1)}$=(α-1/2)δ_0. This wall-to-sphere overlap would push the sphere 1 to move rightward to the new position: $x_1^{(2)}$=-r+($\beta\alpha$-1)(1/2-α)δ_0 and new overlap between two spheres appear. If the algorithm is convergent, it is required that the new overlap be smaller than the initial overlap, therefore it has $x_1^{(2)}<x_1^{(1)}$. After simple calculations, one obtains:

$$\alpha < \alpha_c = \frac{1}{\beta} + \frac{1}{2}. \tag{8}$$

It is worth to mention that from Eq. (8), the initial overlap does not have impact on α_c, which makes this result quite meaningful for 1-D situation. Fig. 3 show these behaviors during the packing process at the values of β=4 and α_c=0.75. These results directly verify the prediction by Eq. (8).

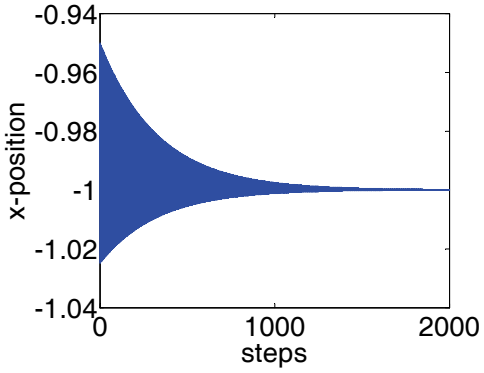

(a) α = 0.749

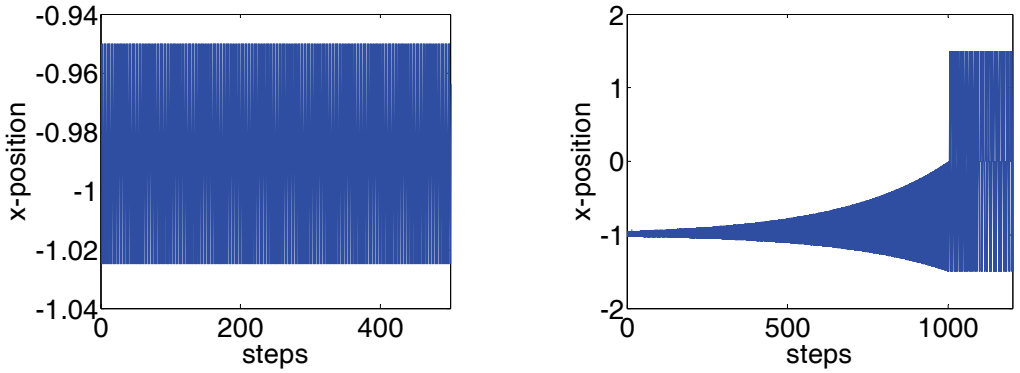

(b) $\alpha = 0.750$ (c) $\alpha = 0.751$

Fig. 3. The motion of Sphere 1 with respect to different α (symmetric initial condition under FBC). The initial perturbation is δ_0=0.1 and the initial gamma value is 0.5.

Now, the mode B is analyzed. For spheres 1 and 2, assuming that their initial positions are $x_1^{(0)}$ and $x_2^{(0)}$, and that their positions after one cycle are $x_1^{(4)}$ and $x_2^{(4)}$, it can be seen that, by following the QDM approach,

$$\begin{aligned} x_1^{(0)} &= -r + \gamma\delta_0, \\ x_1^{(4)} &= \delta_0\gamma - 2\alpha\delta_0 - r + 2\alpha^2\delta_0 + \alpha^2\beta\delta_0 - \alpha^3\beta\delta_0 - \alpha^2\beta\delta_0\gamma, \\ x_2^{(0)} &= r - (1-\gamma)\delta_0, \\ x_2^{(4)} &= r - \delta_0(1-\gamma) + 2\alpha\delta_0 - 2\alpha^2\delta_0 - \alpha^2\beta\delta_0 + \alpha^3\beta\delta_0 + \alpha^2\beta\delta_0\gamma - \alpha\beta\delta_0(\alpha+\gamma-1). \end{aligned} \tag{9}$$

The necessary condition to sustain a strictly periodical mode B motion is:

$$\begin{cases} x_1^{(0)} = x_1^{(4)} & (a) \\ x_2^{(0)} = x_2^{(4)} & (b) \end{cases} \tag{10}$$

The only meaningful solution for Eq. (10) is:

$$\begin{cases} \gamma_c = \dfrac{2}{3} + \dfrac{2}{3\beta} \\ \alpha_c = \dfrac{1}{3} + \dfrac{4}{3\beta} \end{cases} \tag{11}$$

where γ_c is the value of γ under the critical stable condition. It can be seen that, under critical condition, γ and α are only determined by β, which is the relative wall stiffness. For any initial γ that is not equal to γ_c, the system cannot maintain the stable mode B and, instead, it follows mode B, while the γ value converges to γ_c.

When β=4, α_c=2/3, and this analytical result can be verified by Fig. 4. It is also verified by Eq. (11) that initial overlap and γ do not have impact on α_c.

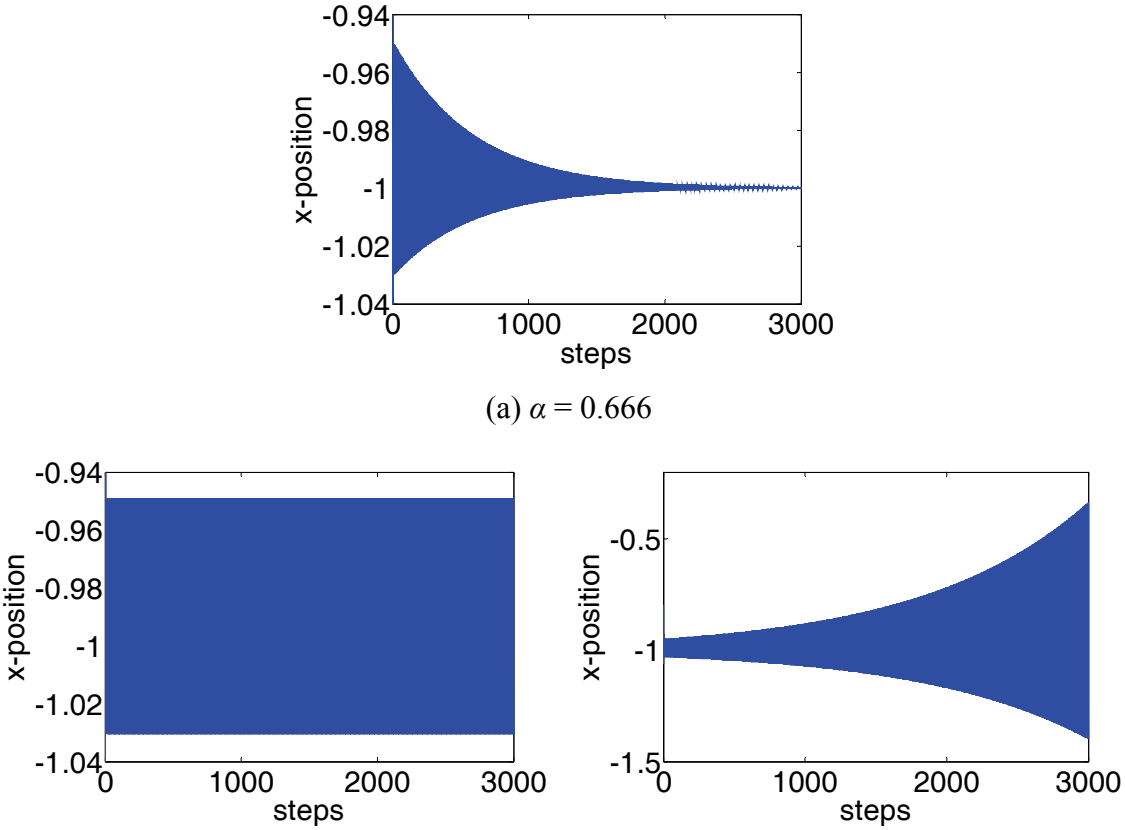

(a) $\alpha = 0.666$

(b) $\alpha = 2/3$

(c) $\alpha = 0.667$

Fig. 4. Motion of Sphere 1 with respect to different α (asymmetric initial condition under FBC). The initial perturbation is δ_0=0.1 and the initial gamma value is 0.5.

Eqs. (8) and (11) provide a stability range for the parameter α, meanwhile, they set up the relationship between the parameter β and the critical value α_c. If $\alpha<\alpha_c$, the system is convergent. If $\alpha=\alpha_c$, the system is stable but not convergent. Both spheres will move back and forth and the overlap is constant. If $\alpha>\alpha_c$, two spheres will swap position or even have infinite displacement no matter how small δ_0 is, hence the system is unstable. Also, Eqs. (8) and (11) imply that greater β (relative wall-to-sphere stiffness) leads to smaller value of α_c. This can be understood by noting that a harder wall can bounce the sphere back further causing larger overlaps with other spheres if α is too large. A small value of α can prevent such a large displacement from the wall, so the stability range of α becomes smaller.

From Eq. (11) it can be seen that, similar to the symmetric case indicated by Eq. (8) (γ=0.5), the value of α_c for FBC and asymmetric packing is independent of the initial overlap. From Eq. (11) it can be observed that the value of γ_c under the critical condition is also fixed, independent of the initial γ value. These observations make the result valid for all initial conditions. The α_c value obtained from symmetric case is a trivial solution, which can only be achieved when the initial γ exactly equals to 0.5. For all other general situations, they might start with mode A, but will eventually follow mode B, where asymmetric case results should be valid.

The critical step size value for the periodic boundary 1-D system can also be determined following the similar procedure as the fixed boundary system. Figure 1b shows the system configuration, which corresponds to an infinite close packing system. Under periodic boundary conditions, only sphere-to-sphere overlap exists, hence the parameter β has no impact on the algorithm performance. By using the same approaches as in the derivation of Eq. (8), one can obtain the critical value α_c for the PBC system:

$$\alpha_c = 1. \tag{12}$$

This result is independent of the initial overlap and the initial γ value, which is numerically verified by Fig. 5.

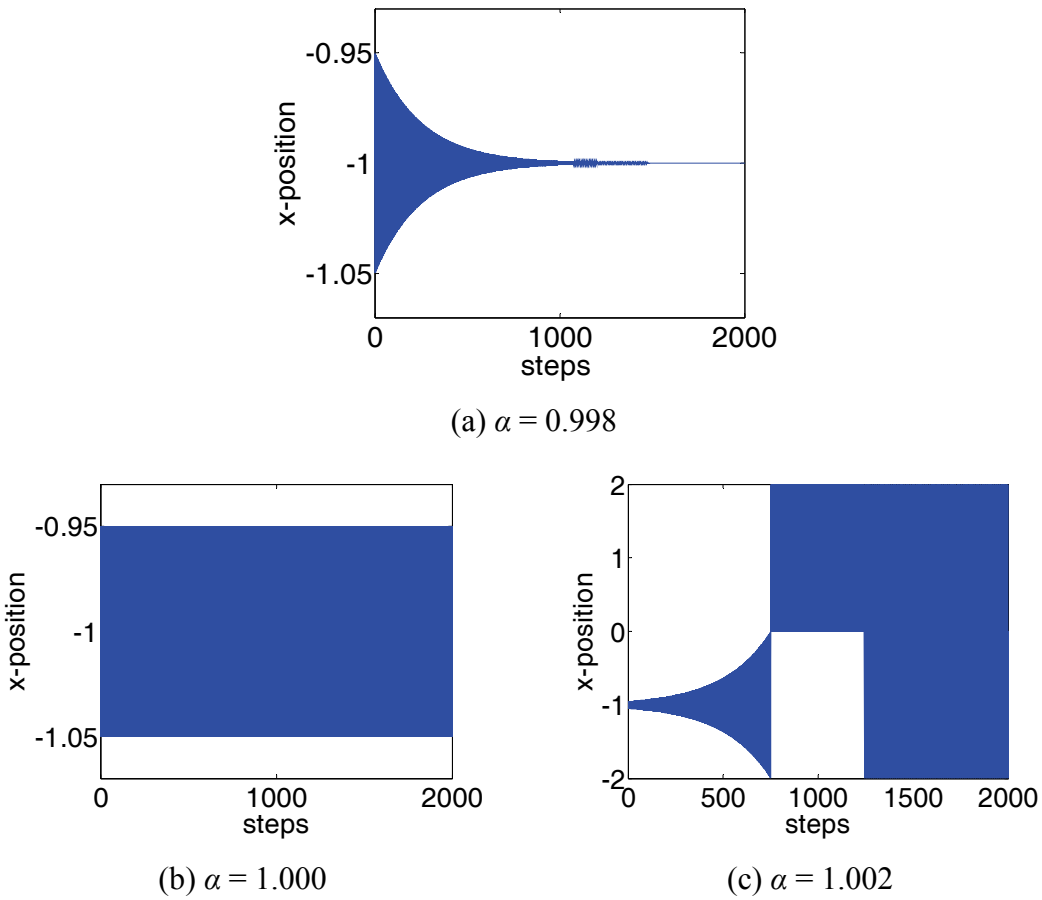

(a) α = 0.998

(b) α = 1.000

(c) α = 1.002

Fig. 5. Position history of sphere 1 under PBC. The initial perturbation is δ_0=0.1 and the initial gamma value is 0.5.

Now, it can be concluded that, for close packing in finite 1-D geometry which lies between Figs. 2a and 2b, there should be $\alpha < \alpha_c \in (\frac{1}{3} + \frac{4}{3\beta}, 1)$ that exists to guarantee the stability of the algorithm. This conjecture can be numerically verified by Fig. 6, where many spheres are horizontally packed in a 1-D system: for 1-D close packing, the value of α_c goes up as the

geometry size (or number of spheres) increases. For a large system which is close to the periodic boundary condition, $\alpha_c \rightarrow 1$.

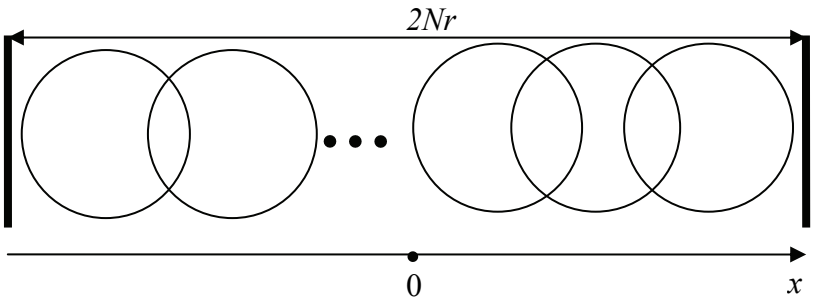

(a) geometry of N-sphere 1-D packing under FBC

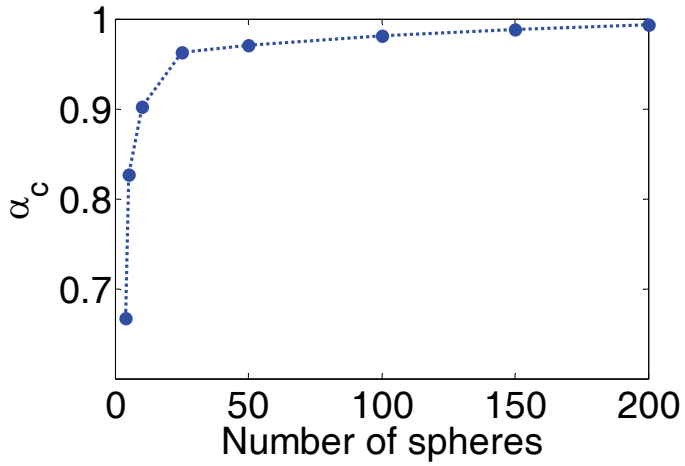

(b) system size (N) impact on α_c

Fig. 6. The relationship between the size of the geometry and α_c in 1-D close packing.

A similar approach can be extended to higher dimension applications. The analysis of a 4-sphere close packing system in 2-D is shown in Fig. 7, where spheres can only move around in a 2-D plane constrained by a rectangular container. The periodic boundary condition defined for Fig. 7c means that once a sphere partially or totally moves out of the boundary (such as the upper bound of x-direction), the corresponding part of the sphere will re-appear from the opposite boundary in the same direction (the lower bound of x-direction). In Fig. 7, the origin of the coordinate system is the center of the container.

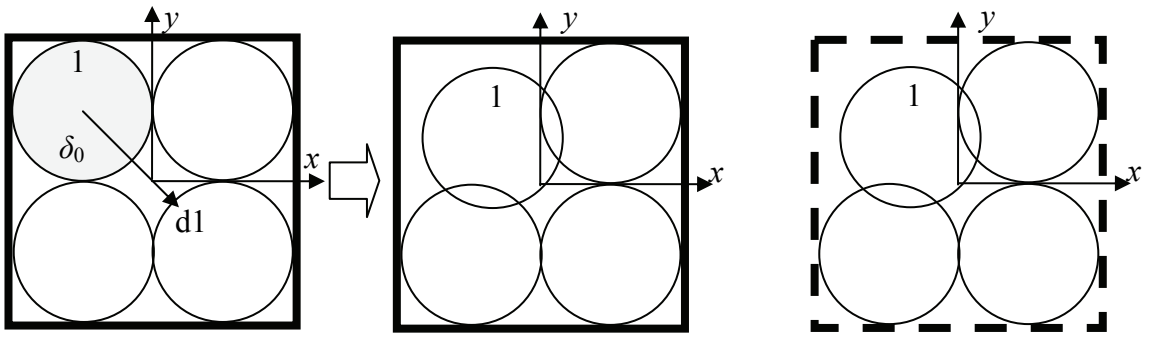

(a) equilibrium state (FBC) (b) perturbed packing (FBC) (c) perturbed packing (PBC)

Fig. 7. Close packing in a rectangular domain with FBC and PBC.

In this 2-D example, assume the radius of the sphere is r=1, then the container has a side length of 4, and the resulted packing fraction is 78.54%. As what we have done for the 1-D system, we perturb one sphere by δ_0 along direction d1, which is 135 degree from the positive direction of y-axis, and obtain a perturbed system in Fig. 7b. Then we apply the QDM to eliminate overlaps by this perturbation, and track the motion of the spheres until they return to the initial configuration, which need more steps compared with 1-D situation. We find that for fixed boundary condition, the spheres follow a similar mode B motion as in the 1-D case. Similar to the theoretical analysis for 1-D case, by comparing the new overlap for the perturbed sphere after one motion cycle with the initial overlap and enforcing the new overlap less than the old one, the upper limits for the control parameter α can be calculated as $\alpha_{c1} = \frac{1}{3} + \frac{4}{3\beta}$, which can be verified numerically by Fig. 8. For any sphere, its x-position and y-position will converge to a fixed position within the container if and only if QDM is convergent. Based on this reason and for simplicity, we only show the x-position history of the perturbed sphere. In Fig. 8a, we set α =0.666, slightly less than 2/3 (α_{c1}) and we can see that the system is convergent. In Fig. 8b, we set α=0.667, slightly larger than 2/3 and we can see that the system is divergent. Figs. 8a and 8b show that the critical step size is between 0.666 and 0.667, which validates the theoretical prediction. The theoretical prediction of the critical step size can be further verified to be independent of both magnitude and direction of the initial perturbation via numerical evaluations. Figure 8c show that the critical step size is constant for all the tested perturbation vectors.

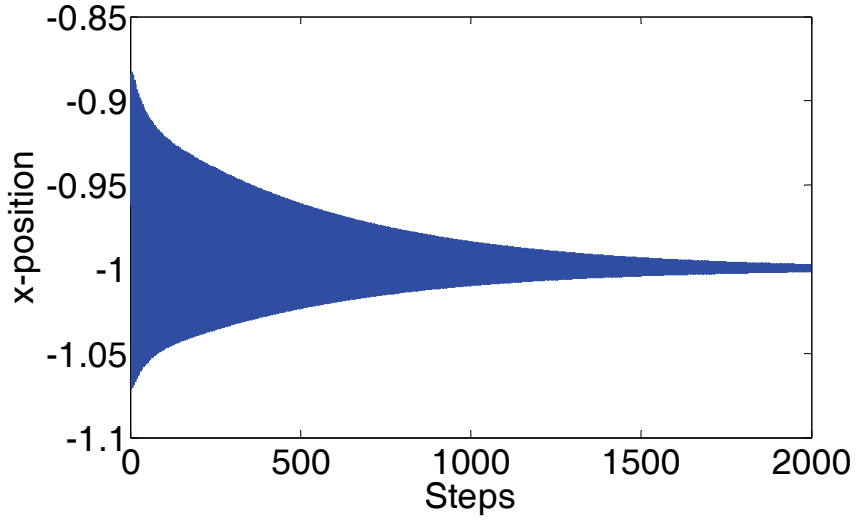

(a) x-position history of sphere 1: Fixed boundary condition, α=0.666, δ_0=0.1r and the algorithm is convergent

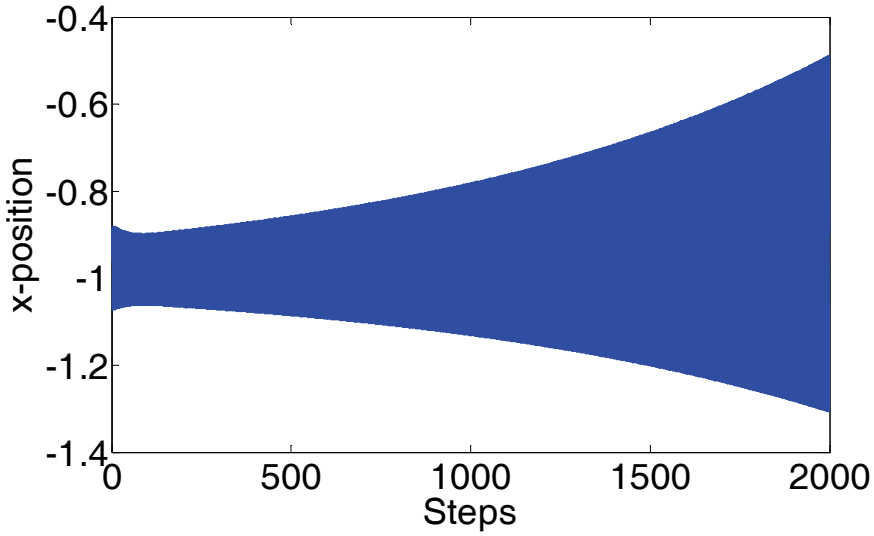

(b) x-position history of sphere 1: Fixed boundary condition, α=0.667, δ_0=0.1r and the algorithm is divergent

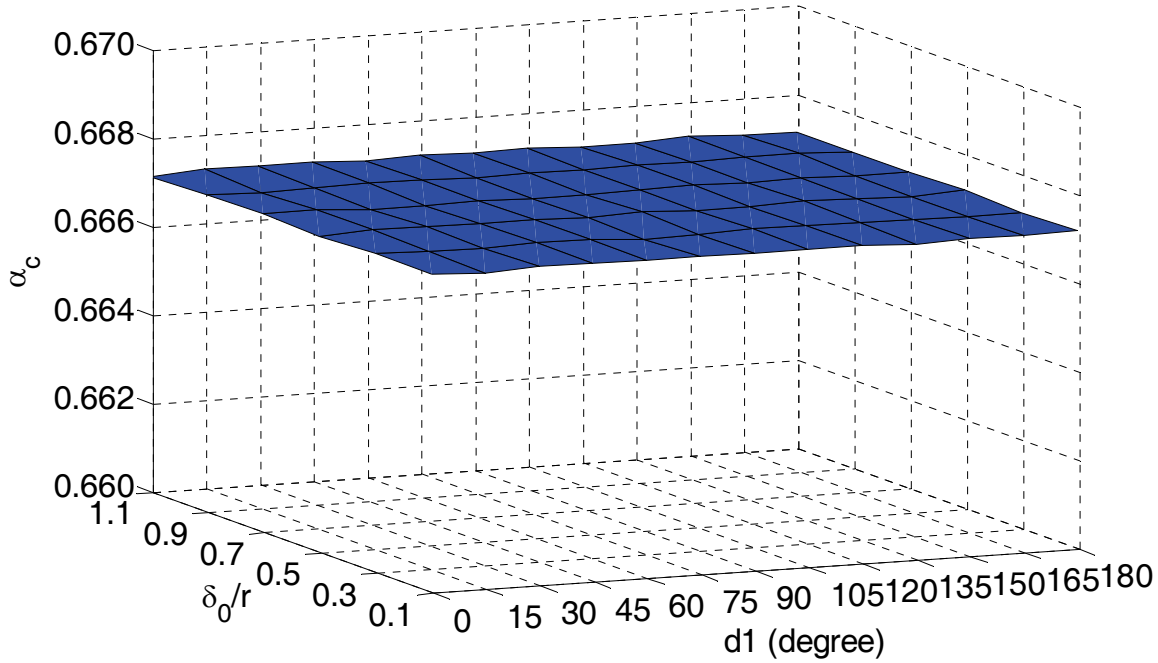

(c) Critical step size for different perturbation angle and magnitude

Fig. 8. Verification of analytical formula for critical step size α_c in a 2-D close-packing domain with the fixed boundary condition (β=4).

For periodic boundary condition, the sphere motion is much more complicated and there is no general mode to follow. The critical step size is affected by both the initial overlap and perturbation direction, which can be seen from Fig. 9. In Fig. 9a, the perturbation direction is fixed at 135 degree, and different perturbation magnitudes are numerically tested. In Fig. 9b, the perturbation magnitude is fixed at δ_0=0.1r, and different perturbation directions are numerically tested. The minimum value for the critical step size is demonstrated to be 1. As a conservative estimation, despite of influences from the perturbation magnitude and direction, we conclude that $\alpha_{c2} = 1$, which corresponds to the perturbation along direction d1 shown in Fig. 7a. In practice, the step size value α should be chosen less than 1.

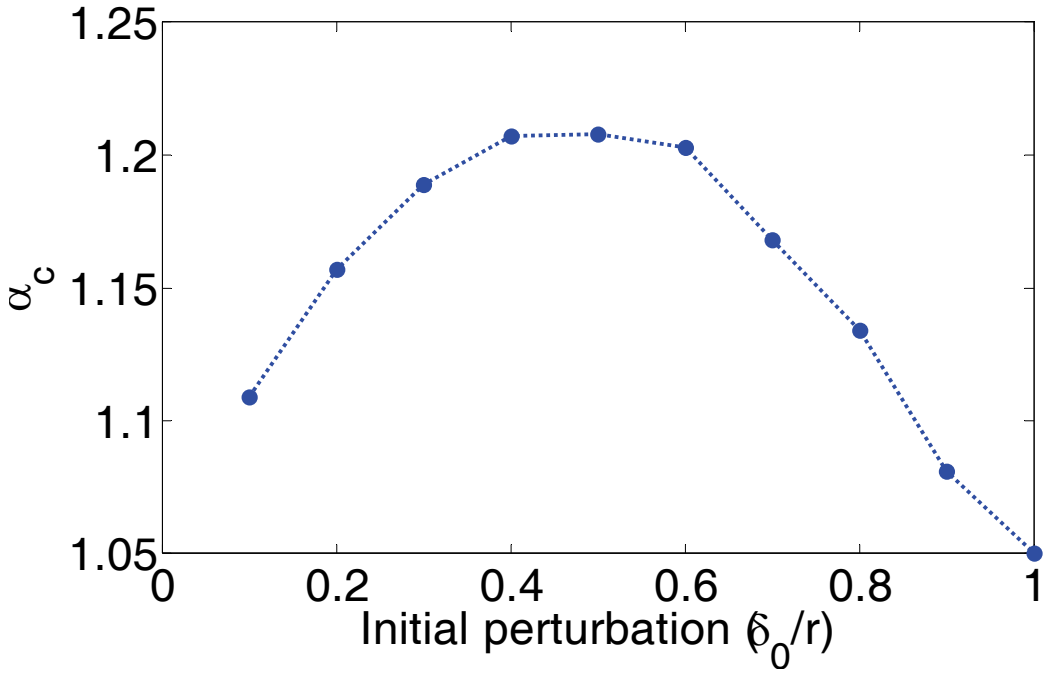

(a) Critical step size as a function of initial perturbation magnitude at the fixed perturbation direction of d1=135 degree

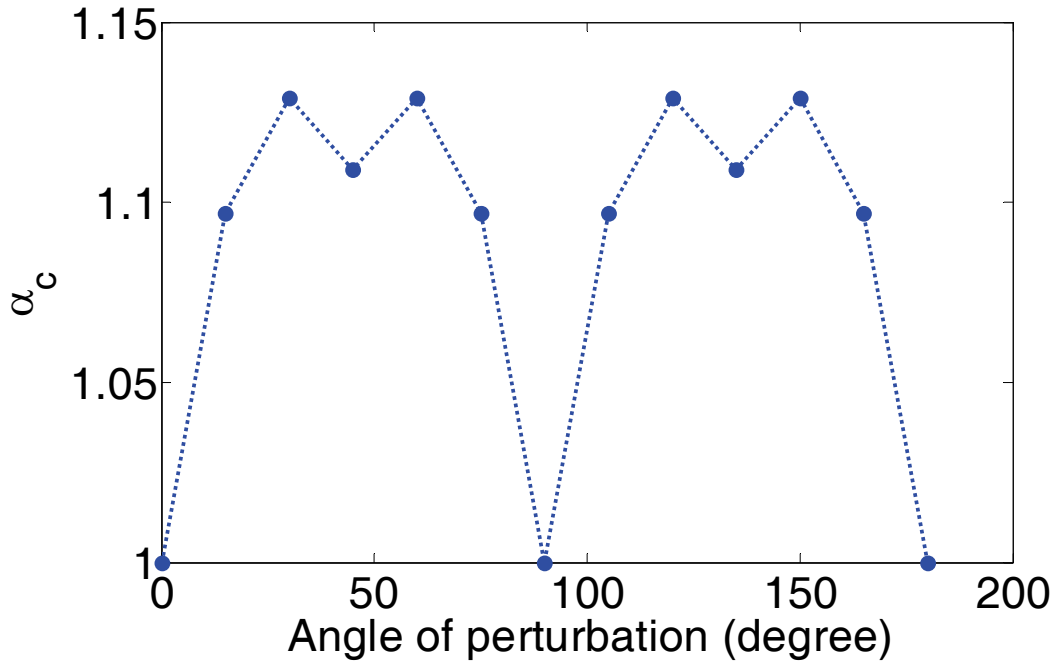

(b) Critical step size as a function of perturbation direction at the fixed perturbation magnitude of δ_0=0.1r

Fig. 9. Impacts of initial perturbation magnitude and direction on the control parameter for 2-D packing with the periodic boundary condition.

By comparing with 1-D results, it can be seen that the critical value of α for both fixed

boundary system and periodic boundary system in 2-D is approximately the same as those for the 1-D situation. It can be concluded that, although there is more complexity for the 2-D case, such as in the initial overlap impact and overlap direction impact, the estimated range of control parameter is similar to the 1-D case.

For a 3-D system, it is harder to obtain exactly quantitative influence of control parameters due to a further increase of degrees of freedom for sphere motion. However, based on 1-D and 2-D observations, we can expect similar stability behavior for a general 3-D situation. Specifically, for a closely packed 3-D system with a general finite geometry, it lies between the smallest possible packing system and an infinite geometry system. Hence, the value of α_c is also expected to approximately have the range [1/3+4/(3β), 1], which is bounded by the value from the smallest and the largest (infinite) domains in 1-D geometry. A numerical experiment for a packing system in cylindrical geometry is performed to verify this upper limit for α. The geometry of the problem originates from the HTR-10 configuration [25]: the cylindrical container has a height H_c=180cm and a radius R_c=90cm, as shown in Fig. 10a. A total of about 24,726 spheres at the radius of r=3cm are packed inside the container, having a packing fraction of *frac*=0.61. The stop criterion is set so that the maximum overlap is less than $10^{-5}r$. It costs about 150 second computation time for every 1000 iteration steps on a Pentium IV 3GHz CPU PC.

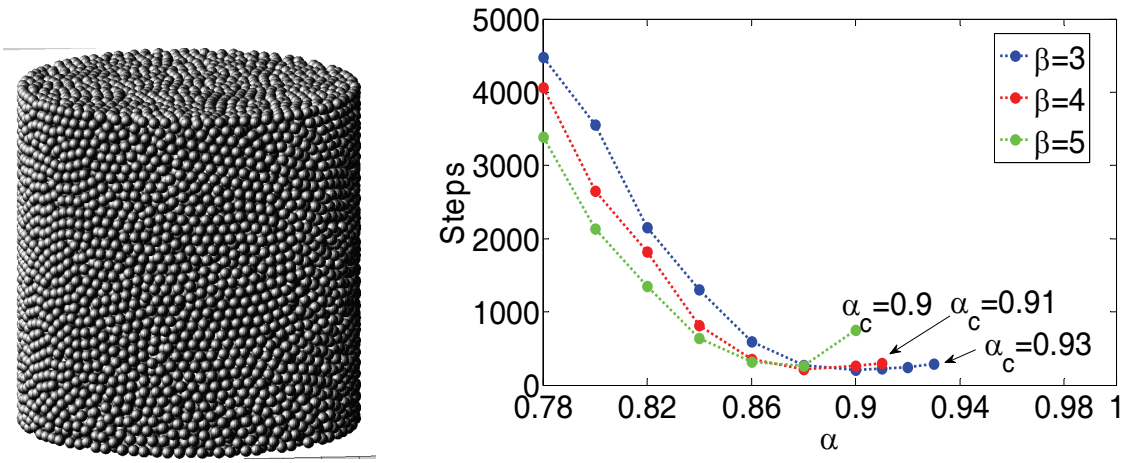

(a) Cylindrical geometry (b) Parameter impact on convergence

Fig. 10. Impacts of the control parameters on the QDM convergence performance.

Figure 10b shows the impact of α and β on the iteration steps that are needed to satisfy the convergence criterion. Three different values of β are used for a series of numerical testing at different values of α up to a critical value. Iteration steps are plotted as a function of α. The critical step size α_c is determined by increasing α at a small increment (0.01) until divergence appears. The value of α corresponding to a step right before divergence occurs is considered to be the critical value, which is marked at the right end of each curve. It can be observed that, as expected, the algorithm efficiency increases as α increases. Also, an increase in the β value leads to a faster convergence but a smaller α_c, which is consistent with the prediction by Eqs.

(8) and (11). For a fixed value of β, optimal α^* exists as α approaches α_c. After this optimal value, curves uptick more or less. This is why we see the increase at the end of each curve. This phenomenon is more prominent for β=5. For the 61% packing shown in Fig. 10a, there are about 20,000 contacting sphere pairs and only 600 wall contacts, therefore this packing is close to the infinite geometry, which accounts for the fact that α_c is close to 1. In practice, in order to achieve high efficiency, the value of α should be set close to α_c. Meanwhile, due to the small impact from the uncertainty in the initial overlapped configuration which is generated by a uniform random sampling procedure, a certain stability margin (α_c-α≈0.2) should be kept in order to maintain the algorithm robustness.

4. Packing Fraction Impact on the QDM Convergence

Besides system geometry and boundary condition, the packing fraction can also affect the critical value of control parameters and, consequently, the QDM convergence. Taking a 1-D loose packing system as an example (Fig. 11), and by following a similar procedure as in the derivation of Eq. (8), we find α_c=1/β+1/2+ε, where ε is the porosity of the system. Therefore a higher packing fraction (lower porosity) will lead to a lower value of α_c.

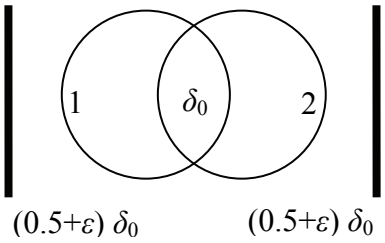

Fig. 11. 1-D loose packing with system width 4r-δ_0.

The impact from packing fraction is especially significant when the system is close to the random close packing state, where sphere jamming may occur. Sphere jamming can significantly deteriorate the convergence performance. For example, Figure 12 shows a possible scenario of a jammed state when three spheres are packed in a 3-D system. This implies that when the QDM is applied to packing spheres, even if the control parameters are chosen to be less than critical values, an overlapped configuration might exist so that the net force on any sphere is zero. According to Eq. (5), QDM will not be able to proceed and all the spheres will remain still. Such a configuration is a jammed state and a random vibration is generally needed, as an addition to the general QDM procedure, to shift the system out of this state. In practice, however, a global jammed state as shown in Fig. 12 is hardly observed for a finite packing system at the packing range that the QDM can handle, though it is observed that the closer to the random close packing, the lower the convergence rate is. The slower convergence can be attributed to the presence of local jamming, where a few spheres may be jammed together. The QDM needs to take more iteration steps to "dissolve" these local jamming.

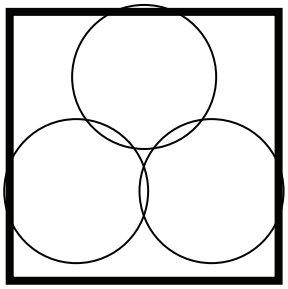

Fig. 12. A jammed packing state.

In order to better illustrate the impact from packing fraction and sphere jamming on QDM convergence, a system energy concept is defined. As mentioned in section 2, the overlap among spheres can be regarded as a compressed spring system. It can be assumed that certain "potential energy" is stored for each overlap. During the iteration, the overlaps for each sphere are changing, so the total "potential energy" for the packing system is changing. If the total "potential energy" shows a global decrease as the overlap elimination is performed iteratively, the algorithm is considered to be convergent. When overlaps are completely eliminated, the total "potential energy" becomes zero. Understanding the random packing process from the "energy" perspective can help analyze and understand the stability and convergence of the QDM. Based on the linear contact repulsive force model described in Eqs. (6) and (7), the step-dependent total "potential energy" for the packing system can be defined as:

$$V^{(k)}(\boldsymbol{X}^{(k)}) = \sum_{i=1}^{N}\sum_{j=1}^{M}\left(\delta_{\mathrm{ij}}^{(k)}\right)^2 + \beta\sum_{i=1}^{N}\left(\delta_{\mathrm{wi}}^{(k)}\right)^2 \geq 0, \tag{13}$$

where $\boldsymbol{X}^{(k)} = [\boldsymbol{X}_1{}^{(k)\mathrm{T}} \quad \boldsymbol{X}_2{}^{(k)\mathrm{T}} \quad ...\boldsymbol{X}_{\mathrm{N}}{}^{(k)\mathrm{T}}]^{\mathrm{T}}$, and $\delta_{\mathrm{ij}}^{(k)}$, $\delta_{\mathrm{wi}}^{(k)}$ are regarded as the magnitude of the contact force at k$^{\mathrm{th}}$ step.

When the system is overlap free, the total "potential energy" becomes 0, i.e. $V(\boldsymbol{X}^*) = 0$. Therefore $V(\boldsymbol{X})$ can be used to measure the overall overlap of the system.

However, according to Eq. (5), neither $\delta_{\mathrm{ij}}^{(k)}$ nor $\delta_{\mathrm{wi}}^{(k)}$ has a direct impact on the move direction and step length of sphere i, instead it is the net force acted on the sphere i that determines its move.

By denoting $\boldsymbol{\delta}_i$ as the vector summation of all inter-sphere overlaps with i$^{\mathrm{th}}$ sphere, we have:

$$\boldsymbol{\delta}_i = \sum_{j \in M_i} \delta_{\mathrm{ij}} \boldsymbol{n}_{\mathrm{ij}} = \boldsymbol{F}_{\mathrm{i}}. \tag{14}$$

Then Eq. (5) can be further simplified as:

$$\Delta \boldsymbol{X}_i = \alpha(\boldsymbol{F}_i + \boldsymbol{W}_i) = \alpha\left(\boldsymbol{\delta}_{\mathrm{i}} + \beta \boldsymbol{\delta}_{\mathrm{wi}}\right), \tag{15}$$

From Eq. (15), it can be observed that the equilibrium of the system is achieved when $\boldsymbol{\delta}_{\mathrm{i}} + \beta \boldsymbol{\delta}_{\mathrm{wi}} = 0$ for all i=1, 2,…,N, which can be equivalent to:

1) $\boldsymbol{\delta}_{\mathrm{i}} = 0,\ \boldsymbol{\delta}_{\mathrm{wi}} = 0$, for all i, or

2) $\boldsymbol{\delta}_{\mathrm{i}} \neq 0,\ \beta \boldsymbol{\delta}_{\mathrm{wi}} \neq 0,\ \boldsymbol{\delta}_{\mathrm{i}} + \beta \boldsymbol{\delta}_{\mathrm{wi}} = 0$, for all i.

In case 1), V=0, therefore the system is overlap free (convergent) and for case 2), V>0, so the system is not convergent. This equilibrium state with non-zero overlaps can be referred to as a jammed state.

When the QDM is applied to the system, it is minimizing the overall magnitude of the net force, which is represented by $U = \sum_{i=1}^{N} \left\| \boldsymbol{\delta}_{\mathrm{i}} + \beta \boldsymbol{\delta}_{\mathrm{wi}} \right\|^2$, instead of minimizing the overall overlap of the system, which is represented by the system potential energy, $V(\boldsymbol{X})$. As long as the system is not in a jammed state, there is

$$U = 0 \Leftrightarrow V = 0, \tag{16}$$

which can be verified by applying a typical QDM procedure to packing a total of 25,000 spheres within a spherical container at the volume fraction packing of 63%, as shown in Fig. 13. In this application, the spheres have a uniform radius of 2cm, and the container is 136.5cm in diameter. The algorithm parameters are α=0.88 and β=4.

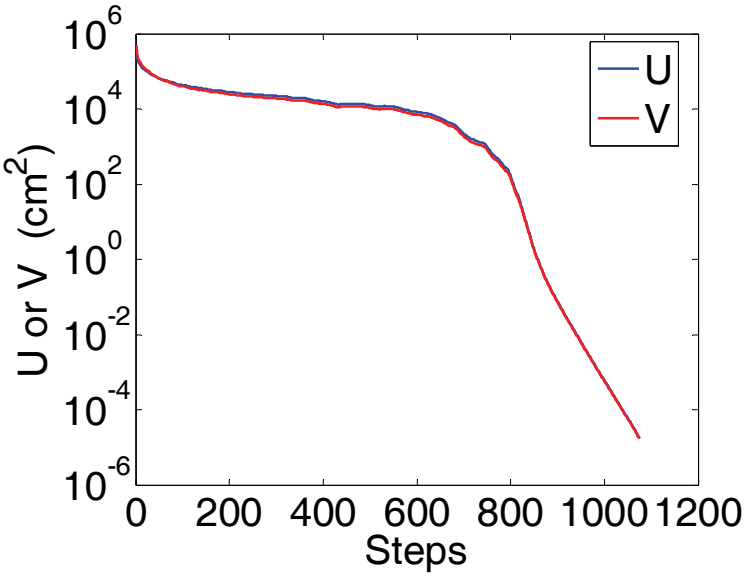

Fig. 13. Typical U and V convergence history.

Based on the definition of overlap potential energy function $V(\boldsymbol{X})$, the convergence rate at the k^{th} step can be characterized by:

$$\rho^{(k)} = \frac{V^{(k)}(\boldsymbol{X})}{V^{(k-1)}(\boldsymbol{X})}. \tag{17}$$

If the QDM is convergent, then the average value of the convergence rate $\overline{\rho^{(k)}} < 1 \text{as } k \to \infty$,

where $\overline{\rho^{(k)}} = \frac{1}{k}\sum_{l=0}^{k} \rho^{(l)}$.

In order to quantitatively investigate the packing fraction impact on the QDM convergence performance, the same cylindrical geometry as shown in Fig. 10a with four different packing fractions are studied (Fig. 14). In all the cases, we use the same settings of the control parameters: α=0.87 and β=4. The maximum and average overlap size, as well as the convergence rate defined by Eq. (17), are plotted as a function of iteration step k.

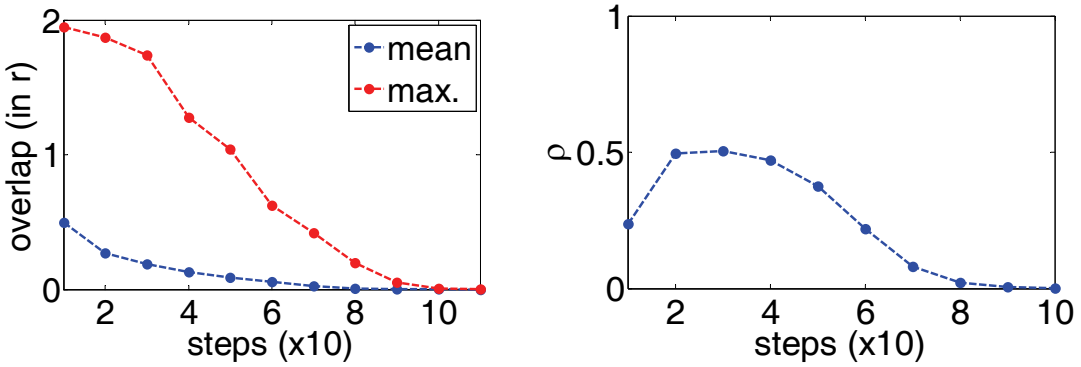

(a) *frac*=0.58

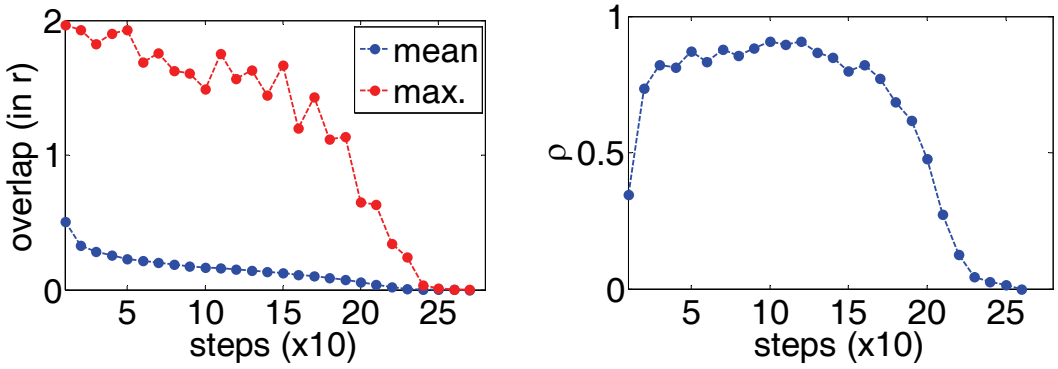

(b) *frac*=0.61

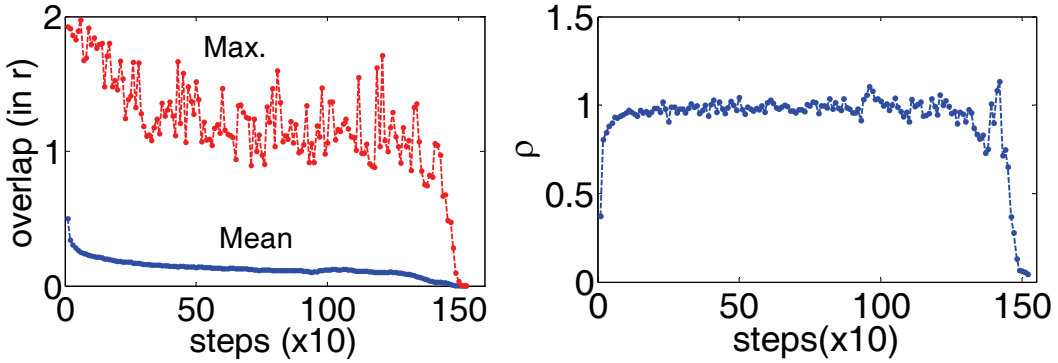

(c) *frac*=0.625

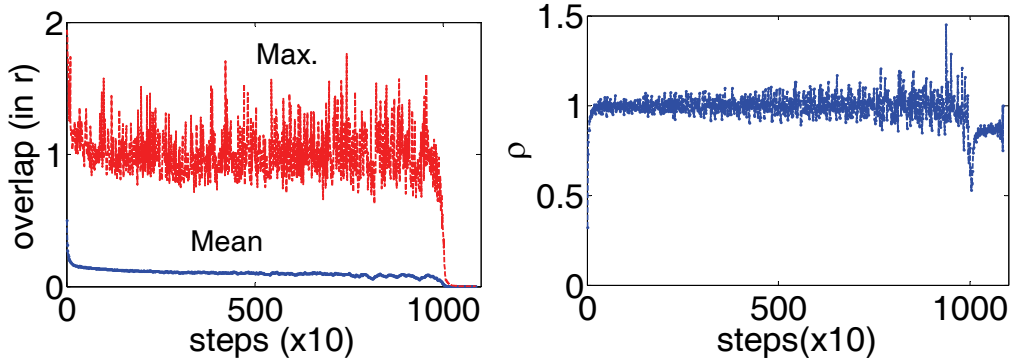

(d) *frac*=0.635

Fig. 14. QDM convergence performance for different packing fractions.

From Fig. 14, it can be seen that, for a large cylindrical geometry, QDM can handle the packing fraction up to around 64%, which approximately corresponds to the random close packing (maximum jamming state). For the loose packing at 58% and 61%, as shown in Figs. 14a and 14b, the convergence criterion (ρ<1) can be strictly satisfied for every step. As packing fraction increases above 62.5%, local jamming starts to form and ρ will sometimes be greater than 1. However, since the average convergence rate $\bar{\rho}$ is less than 1, the system can still converge to an overlap-free configuration. For high density packing (*frac*=63.5%) near the random close packing state, where local jamming widely exists, QDM convergence rate fluctuates around 1 and a considerably long time is needed to converge. For a packing fraction that is even higher, multiple vibrations are needed to shift the spheres out of the jammed state. Moreover, the α_c corresponding with each packing fraction (from 0.58 to 0.635)

are 0.93, 0.91, 0.90 and 0.87. These values of α_c are determined by a series of numerical testing, i.e. increase the value of α by an increment of 0.01 until divergence appears. The value of α that corresponds to the value right before the divergent state is considered to be α_c. It can be seen that as the packing fraction increases, α_c decreases, which is consistent with the estimations from the 1-D/2-D situations. In practice, for higher packing fractions, the value of α should be reduced accordingly in order to maintain the stability margin. It should be noted that smaller value of ρ corresponds with faster convergence, and for a fixed step size, the moving distance for each overlap is proportional to the overlap size. At the initial stage of overlap elimination, the uniformity of inter-sphere overlap distribution is relatively low, and the system potential is dominated by a few of large overlaps, which will be reduced quickly. After the initial stage, the spheres are evenly distributed with moderate overlaps and for most inter-sphere overlaps, the reduction of a certain overlap will result in a new overlap with other spheres, hence the system potential reduction rate (convergence speed) is slowed down. At the final stage, most of the inter-sphere overlaps have already been eliminated and only a few small overlaps exist, the reduction/elimination of these small overlap will be unlikely to bring in new overlaps with other spheres, hence the convergence speed will increase again. For the case of *frac*=63.5%, it is very close to the random close packing limit, and even for small overlaps the reduction/elimination will still cause new overlaps with other spheres, therefore the convergence speed does not drop much, which corresponds to a higher value of ρ.

5. Conclusions

The original Quasi-Dynamics Method (QDM) is reformulated into a simplified version with two control parameters, the relative wall-to-sphere stiffness β and the step size α. Since the wall stiffness β is usually fixed at a value reflecting the realistic material properties, the only major concern of algorithm parameter impact on stability is the step size α. Analytical results from extreme 1-D and 2-D situations show that for a fixed value of β, the upper limit for the step length has a range between $1/3+4/(3\beta)$ and 1 from the smallest domain to the largest (infinite) domain. The initial sphere positions and overlap alignment do not have noticeable impacts on the QDM stability in both 1-D and 2-D cases. For the 3-D situation, it is difficult to obtain similar analytical estimations, a numerical analysis is performed to verify the prediction that the step size α still lies within the same range. For a packing domain at a large size, such as the Pebble Bed Reactor core, α_c is close to the infinite geometry situation, where α_c is close to 1. The most important observation from the numerical analysis in 3-D geometry is that, in order to achieve high efficiency, α should be close to α_c. Simultaneously, some margin should be kept in order to account for the impact from the uncertainty of the initial random position sampling. The impact of β is also investigated, which shows that larger β leads to a smaller α_c, hence smaller stability margin. This observation agrees with the simulation results from the prediction in 1-D analyses. The packing fraction also has impact on the control parameters, in which higher packing fraction brings down the value of α_c, as predicted by extreme 1-D situation and numerically verified by 3-D simulation.

A system “energy potential” concept is proposed to measure total overlaps of the system including inter-sphere overlaps and sphere-wall overlaps. By investigating the QDM formulation, it is shown that the driven factor for the QDM convergence is the net force (vector summation of overlaps) on each sphere, not the magnitude of specific inter-sphere or sphere-wall overlaps. Near random close packing, which pertains to a packing fraction around 64%, local jamming or global jamming will form which can lead to zero net force but non-zero overlap potential. Using this information, it is inferred that the highest packing fraction that QDM can handle is around 64%. This conjecture is justified by applying the algorithm to the pebble packing in PBR geometry with different packing fractions. The convergence performance shows that the algorithm indeed can handle up to the RCP limit. For higher packing fractions, due to the wide existence of local jamming or even strict global jamming, QDM may stay at the jammed state. Therefore, other auxiliary techniques, such as vibrations, are needed to shift the system out of the jamming state.

Acknowledgement
This work was performed under the auspices of the U.S. Nuclear Regulatory Commission Faculty Development Program under contract NRC-38-08-950.

References
[1] K. Bagi, An algorithm to generate random dense arrangements for discrete element simulations of granular assemblies, Granular Matter, 7 (2005) 31-43.
[2] J.-F. Jerier, D. Imbault, F.-V. Donze, P. Doremus, A geometric algorithm based on tetrahedral meshes to generate a dense polydisperse sphere packing, Granular Matter, 11 (2009) 43-52.
[3] A.M. Ougouag, J.M. Cogliati, J.-L. Kloosterman, Methods for modeling the packing of fuel elements in pebble bed reactors, in: Proceeding of International Conference on Mathematics and Computation, Supercomputing, Reactor Physics and Nuclear and Biological Applications, Palais des Papes, Avignon, France, Sept 12-15, 2005.
[4] C.H. Rycroft, G.S. Grest, J.W. Landry, M.Z. Bazant, Analysis of granular flow in a pebble-bed nuclear reactor, Physical review E, 74 (2006) 021306.
[5] Y. Li, W. Ji, Pebble Flow and Coolant Flow Analysis Based on a Fully Coupled Multi-Physics Model, Nuclear Science and Engineering, 173 (2013) 150-162.
[6] Y. Li, W. Ji, Acceleration of coupled granular flow and fluid flow simulations in pebble bed energy systems, Nuclear Engineering and Design, 258 (2013) 275-283.
[7] J.D. Bernal, J. Mason, Packing of Spheres: Co-ordination of Randomly Packed Spheres, Nature, 188 (1960) 910-911.
[8] G.D. Scott, D.M. Kilgour, The density of random close packing of spheres, Journal of Physics D: Applied Physics, 2 (1969) 863.
[9] J.L. Finney, Random Packings and the Structure of Simple Liquids. I. The Geometry of Random Close Packing, Proceedings of the Royal Society of London. A. Mathematical and Physical Sciences, 319 (1970) 479-493.
[10] W.S. Jodrey, E.M. Tory, Computer simulation of close random packing of equal spheres, Physical Review A, 32 (1985) 2347-2351.
[11] A.S. Clarke, J.D. Wiley, Numerical simulation of the dense random packing of a binary

mixture of hard spheres: Amorphous metals, Physical Review B, 35 (1987) 7350-7356.
[12] G.T. Nolan, P.E. Kavanagh, Computer simulation of random packing of hard spheres, Powder technology, 72 (1992) 149-155.
[13] D. He, N.N. Ekere, L. Cai, Computer simulation of random packing of unequal particles, Physical review E, 60 (1999) 7098-7104.
[14] S. Torquato, T.M. Truskett, P.G. Debenedetti, Is random close packing of spheres well defined?, Physical Review Letters, 84 (2000) 2064-2067.
[15] S. Torquato, Random Heterogeneous Materials: Microstructure and Macroscopic Properties, Interdisciplinary Applied Mathematics, Springer-Verlag, New York, 2002.
[16] S.X. Li, L. Zhao, Y.W. Liu, Computer simulation of random sphere packing in an arbitrarily shaped container, Cmc-Computers Materials & Continua, 7 (2008) 109-118.
[17] C. Song, P. Wang, H.A. Makse, A phase diagram for jammed matter, Nature, 453 (2008) 629-632.
[18] D.W. Cooper, Random-sequential-packing simulations in three dimensions for spheres, Physical Review A, 38 (1988) 522.
[19] G.E. Mueller, Numerically packing spheres in cylinders, Powder technology, 159 (2005) 105-110.
[20] K. Soontrapa, Y. Chen, Mono-sized sphere packing algorithm development using optimized Monte Carlo technique, Advanced Powder Technology, (2013).
[21] Y. Li, W. Ji, A collective dynamics-based method for initial pebble packing in pebble flow simulations, Nuclear Engineering and Design, 250 (2012) 229-236.
[22] A. Sutou, Y. Dai, Global optimization approach to unequal global optimization approach to unequal sphere packing problems in 3D, Journal of Optimization Theory and Applications, 114 (2002) 671-694.
[23] A. Yang, C.T. Miller, L.D. Turcoliver, Simulation of correlated and uncorrelated packing of random size spheres, Physical review E, 53 (1996) 1516-1524.
[24] G. Maess, LaSalle, J. P., The Stability and Control of Discrete Processes. New York etc., Springer-Verlag 1986. VII, 150 pp., 15 figs., DM 49,80. ISBN 3-540-96411-8 (Applied Mathematical Sciences 62), ZAMM - Journal of Applied Mathematics and Mechanics / Zeitschrift für Angewandte Mathematik und Mechanik, 68 (1988) 195-195.
[25] Z. Gao, L. Shi, Thermal hydraulic calculation of the HTR-10 for the initial and equilibrium core, Nuclear engineering and design, 218 (2002) 51-64.